ELSEVIER

European Journal of Pharmacology 322 (1997) 249–257

ejp

Heterogeneous levamisole receptors: a single-channel study of nicotinic acetylcholine receptors from *Oesophagostomum dentatum*

Richard J. Martin [a,*], Alan P. Robertson [a], Henrik Bjorn [b], Nicholas C. Sangster [c]

[a] *Department of Preclinical Veterinary Sciences, R.(D.)S.V.S., Summerhall, University of Edinburgh, Edinburgh, EH9 1QH, UK*
[b] *Department of Pharmacology and Pathology, Royal Veterinary and Agricultural University, Frederiksberg C, Denmark*
[c] *Department of Veterinary Pathology, University of Sydney, Sydney, NSW 2006, Australia*

Received 3 October 1996; revised 13 December 1996; accepted 20 December 1996

Abstract

A muscle vesicle preparation from *Oesophagostomum dentatum*, a 5 mm parasitic nematode, was developed for single-channel recording. Properties of nicotinic acetylcholine receptors activated by the anthelmintic levamisole (10 μM) were investigated using cell-attached and isolated inside-out patches. The current-voltage relationships of the single-channel currents were linear with conductances in the range 24.6–57.7 pS (mean 39.5 pS). The distributions of open times were fitted with a single exponential and mean open times were in the range 0.98–4.43 ms (mean 2.2 ms). The distributions of conductances and open times of the channels showed that the receptors could not be described as a single homogeneous population. There were two main channel subtypes: one subtype, designated *G35*, had a mean conductance of 35.2 pS and mean open time of 1.6 ms; another subtype, designated *G45*, had a mean conductance of 44.6 pS and mean open time of 2.7 ms. A channel with a conductance near 25 pS, designated *G25*, and a channel with a conductance near 55 pS, designated *G55*, were also observed. The designations were based on the mean conductances, *G*, of the channel subtypes. A model for the heterogeneous population of nicotinic acetylcholine channels predicting four subtypes of receptor separated by their conductance is discussed and related to the development of levamisole resistance.

Keywords: Levamisole; Nicotinic acetylcholine receptor; Heterogeneity; (*Oesphagostomum dentatum*); Patch clamp

1. Introduction

Levamisole is an anthelmintic drug used for the control and treatment of many parasitic nematode infections. The electrophysiological effects of levamisole on nematodes are often studied in the pig intestinal nematode, *Ascaris suum*, because of its availability, large size and close relationship to the human ascariasis parasite. Levamisole acts as a selective nicotinic agonist, producing spastic paralysis of parasitic nematodes but not of the host (Aceves et al., 1970); it produces depolarization of somatic muscle cells by increasing the input conductance of muscle to cations (Harrow and Gration, 1985). Patch-clamp experiments on *Ascaris suum* muscle have demonstrated that levamisole gates nicotinic acetylcholine receptor ion channels that conduct monovalent cations non-selectively with single-channel conductances in the range 19–46 pS and mean open times in the range 0.8–2.9 ms (Robertson and Martin, 1993).

Resistance to levamisole therapy is now spread widely and a serious problem limiting the treatment of different parasites (Prichard, 1994). Genetic experiments on the model soil nematode *Caenorhabditis elegans* have identified 11 genes involved in producing levamisole resistance and three of these genes, *unc-38*, *unc-29*, *lev-1*, encode subunits of a nicotinic acetylcholine receptor (Lewis et al., 1980; Fleming et al., 1997). The small size of *C. elegans* has so far limited electrophysiological studies and resistant strains of *Ascaris* are not available. To overcome these problems we have selected the nodular worm of the pig, *Oesphagostomum dentatum* (Fig. 1), for further study. *O. dentatum* is a 5 mm intestinal nematode parasite of pigs causing nodular lesions. It may be maintained by cryopreservation of L_3 larvae and experimental infection; anthelmintic-resistant strains of *O. dentatum* are available (Bjorn, 1994).

In this paper we describe a method for recording lev-

* Corresponding author. Tel.: (44-131) 650-6094/5; Fax: (44-131) 650-6576; e-mail: R.J.Martin@ed.ac.uk

0014-2999/97/$17.00
PII S0014-2999(96)00996-X

amisole-activated single-channel currents from membrane vesicles prepared from somatic muscle of *O. dentatum*. We describe some of the properties of the channel currents, revealing heterogeneity of the receptor-operated ion channels, and we discuss a model for this heterogeneity.

2. Materials and methods

2.1. Preparation of adult O. dentatum

At the Royal Veterinary and Agricultural School, Frederiksberg, Copenhagen, 10 000 L_3 larvae were administered by stomach tube to 25 kg Landrace X pigs. Infection was confirmed by faecal egg counts on day 21 after infection. Pigs were slaughtered in the conventional manner by electrical stunning and bleeding out. The adult worms were collected from the large intestine and cleaned using the agar migration technique (Slotved et al., 1996) and then placed in a stainless steel Thermos flask, at 37°C, containing a maintenance solution (composition mM): NaCl, 150; KCl, 2.7; $CaCl_2$, 2; $MgCl_2$ $6H_2O$, 0.3; PIPES, 10; NaOH, 13; glucose, 11; $NaHCO_3$, 12 and penicillin, 0.06 g/l; streptomycin, 0.1 g/l. The adults were shipped overnight by TNT International to arrive the next day in Edinburgh.

At Edinburgh the adult *O. dentatum* were removed from the Thermos flask and placed in Petri dishes containing maintenance solution in an incubator at 20°C. The maintenance solution was changed daily. Under these conditions adult *O. dentatum* survived for 7–14 days.

2.2. Preparation of muscle vesicles

The adult female *O. dentatum* is about 5 mm long, larger than the male (Fig. 1) and is slightly easier to dissect. For some reason unknown to us the females usually survived longer than the males after collection, so we only used the female for preparation of muscle vesicles.

A single female worm was pinned, with small insect mounting pins, through the head and tail in a 2.5 cm Petri dish with Sylgard resin lining the base. The preparation was bathed in solution-1, a low-Ca^{2+} maintenance solution containing (mM): NaCl, 35; Na acetate, 105; KCl, 2; $MgCl_2$, 2; HEPES 10; glucose, 3; EGTA, 1; ascorbic acid, 0.5; adjusted to pH 7.2 with NaOH. Solution-1 is based on *Ascaris* solutions (Martin, 1980) and contains reduced Cl^-.

Under the dissecting microscope a microscalpel, made from a broken razor fitted to a pencil-like holder, was used to cut through the cuticle and body wall on one side into the peritoneal cavity and along the length of the nematode. The preparation was opened out and pinned flat with more small insect mounting pins (Fig. 2A). The preparation was washed and placed in solution-2, containing (mM): NaCl, 35; Na acetate, 105; KCl, 2; $MgCl_2$, 2; HEPES 10; glucose, 3; ascorbic acid, 0.5; collagenase (1 mg/ml) adjusted to pH 7.2 with NaOH and maintained at 37°C. The preparation was maintained in solution-2 at 37°C for 10 min and then washed in solution-1 and again maintained at 37°C. Vesicles (10–50 μm in size) formed over the next hour as outgrowths from the muscle (Fig. 2B). The vesicles were used within the next 5 h.

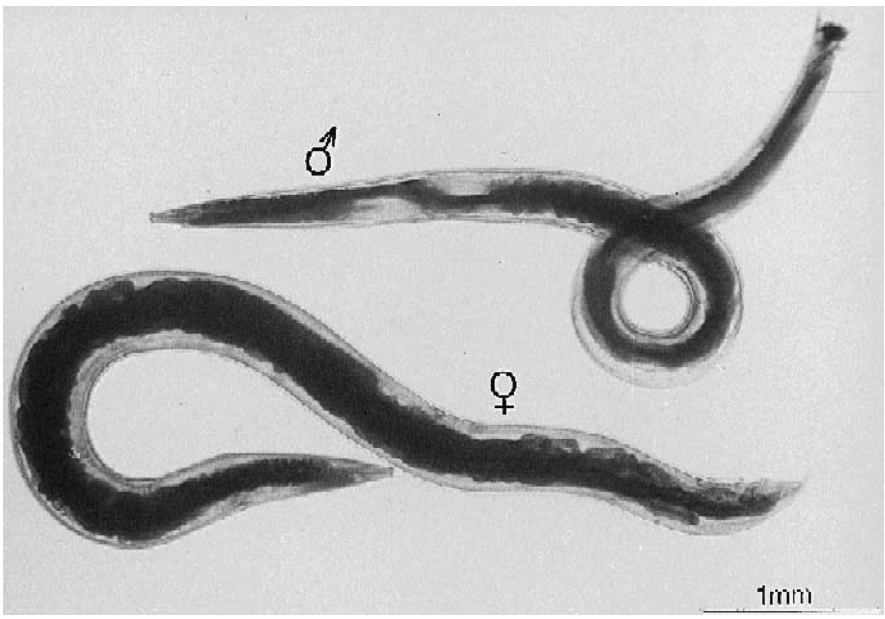

Fig. 1. Photomicrograph of an unstained male (top) and female (bottom) *O. dentatum* after recovery from the intestine of a pig. The female is about 5 mm in length.

2.3. Patch-clamp recordings

Individual vesicles were harvested with the aid of a micropipette with a tip of 100 μm fitted to a microsyringe driver and manipulator. The vesicles were harvested from the flap preparation and transferred to the experimental chamber where recordings were made at room temperature (15–22°C). The experimental chamber was mounted on the stage of a Nikon TMS-PH3 inverted microscope and viewed at ×300 under phase contrast for the patch-clamp experiments (Fig. 2C).

The vesicles were bathed in a high-Cs solution-3, designed to reduce K currents: it contained (mM): CsCl, 35; Cs acetate, 105; $MgCl_2$, 2; dithiothreitol, 0.1; HEPES, 10 and EGTA, 1; pH adjusted to 7.2 with CsOH. Our initial patch recordings were made from preparations that were obtained using solutions without adding dithiothreitol to solution-3 (the bath solution). We found, however, that the patches were often very fragile and broke down easily when potentials exceeding ±50 mV were applied across the patch. We reasoned that the muscle membranes may be oxidized because they were exposed to a higher than normal pO_2 unlike their natural environment in the large intestine. To reduce oxidation, we incorporated 100 μM dithiothreitol in solution-3. We were aware of the possibility of high concentrations of dithiothreitol inactivating nicotinic channels (Kao and Karlin, 1996) so we tried decreasing concentrations of dithiothreitol to determine the lowest concentration that would permit recording of nicotinic channels from stable membranes. As a consequence of adding 100 μM dithiothreitol concentrations to solution-3 we were able to make records of channel activity from patches which were able to resist potentials in excess of ±100 mV.

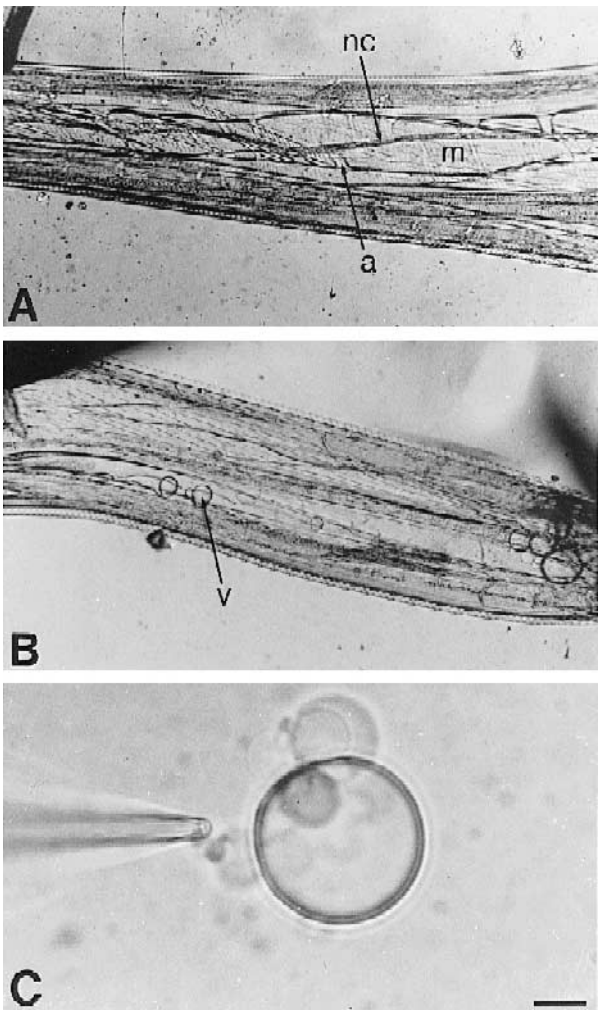

Fig. 2. Photomicrographs of the preparation of muscle vesicles. A: Flap preparation of *O. dentatum* produced by cutting the worm through the cuticle with a microscalpel and pinning it open cuticle side down onto a plate of Sylgard in a small Petri dish. M, muscle cell; a, muscle arm; nc, nerve cord. Magnification ×20. B: Collagenase treatment and incubation results in the appearance of vesicles (V) which bleb off the muscle cell. Magnification ×20. C: Vesicle viewed under phase contrast together with a patch pipette that was approaching the vesicle for recording. Scale bar 10 μm.

Recordings were made using cell-attached patch recordings or isolated inside-out patch recordings. Patch electrodes were made from Garner (7052) capillary glass with a resistance of 1 MΩ. The pipettes were coated on the outside to near their tips with Sylgard to improve the frequency responses. Patch pipettes were filled with solution-4 which was (mM): CsCl, 140; $MgCl_2$, 2; HEPES 10; EGTA, 1; levamisole 0.01; pH 7.2 with CsOH. Solutions-3 and -4 were Ca^{2+}-free to reduce the contamination of patch recordings with Ca^{2+}-activated channels.

2.4. Data processing

Currents were recorded with an Axopatch 200 B and modified Sony digital audioprocessor onto DAT tape. Channel records were analyzed with an Axon Instruments Digidata 1200 A interface, an RM Pentium computer with Pclamp V6.0 software using Fetchan and pSTAT programs. The records were digitally filtered at 1.5 kHz by the software; the sampling time was 25 μs; and the minimum detectable interval was 0.3 ms. The threshold for channel opening was set at 50% of the single-channel amplitude and durations and channel states measured with Fetchan programs with a minimum resolvable interval of 100 μs. pSTAT was used to describe the distributions of the open, closed, and burst times. Exponential curves were fitted to the durations using the non-linear simplex maximum likelihood procedure. Gaussian curves were fitted using non-linear simplex least squares to the distribution of channel current amplitudes to determine the mean channel amplitude at particular potentials. Bursts of openings were defined with a critical gap length set at 3 ms.

The data are expressed as means ± S.E.M. Mean open times, mean conductances of the channel subtypes were compared using a Student's *t*-test (one tail).

2.5. Chemicals

Levamisole hydrochloride, dithiothreitol and collagenase type IA were purchased from Sigma.

3. Results

3.1. Levamisole-activated channels

We selected low-Ca^{2+} and high-Cs^{+} solutions for recording to avoid contamination by Ca^{2+}-activated channels or by Na^{+} or by K^{+} channels. In addition we used symmetrical Cs^{+} but non-symmetrical Cl^{-} concentrations in the bath and pipette to give, in isolated patches, a reversal potential of −33 mV for a Cl^{-}-selective channel and a 0 mV reversal potential for a non-selective cation channel. Under the recording conditions selected we could observe two kinds of channel in cell-attached and isolated inside-out patches.

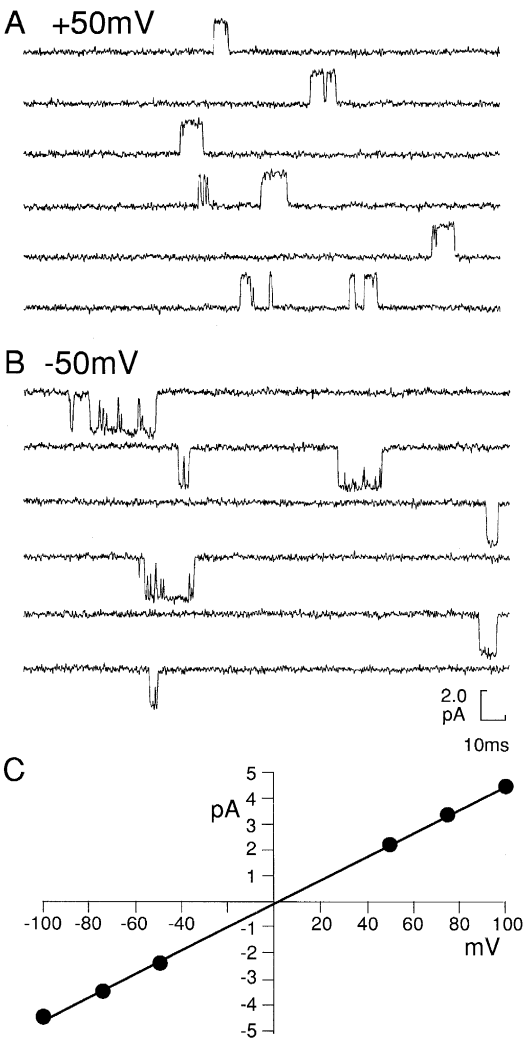

Fig. 3. Nicotinic acetylcholine receptor channel currents at pipette potential, (A) +50 mV and (B) −50 mV in a cell-attached patch. (C) Current-voltage relationship and least-squares fit giving a conductance of 45.1 ± 0.5 pS with a reversal potential close to 0 mV.

The first type, observed occasionally, had a reversal potential near 0 mV in isolated patches, a small (5–10 pS) conductance, and was voltage-sensitive opening more frequently when the patch was depolarized for several seconds. These channel currents were not interpreted as nicotinic channels because they could be recorded in the absence of levamisole in the pipette. They were classified as non-selective cation channels because they had reversal potentials near 0 mV. This channel may underlie a slow non-selective cation current like that recognised in *Ascaris* (Martin and Valkanov, 1996). This kind of channel current was edited out of the current records when necessary.

Fig. 3A and B illustrates representative recordings at +50 mV and −50 mV of the other kind of channel current we saw in the patches. This channel was recognised as the nicotinic acetylcholine receptor because: (1) it was not present if levamisole was not present in the patch pipette; (2) the channel showed little voltage sensitivity, opening at positive and negative membrane potentials; (3) the channel had conductances that ranged between 24–58 pS; (4) the channel had brief openings in the millisecond range. This kind of channel is similar to the nicotinic channel currents of *Ascaris* (Robertson and Martin, 1993). Fig. 3A shows examples of these channel currents recorded from a cell-attached patch recorded with a pipette potential of +50 mV. It can be seen that the currents are brief (millisecond) outward current pulses that have an amplitude of 2.3 pA and they occur in bursts with very brief (approximately 0.3 ms) closings separating the openings of a burst. Fig. 3B shows that at −50 mV, the channel currents are inward with an amplitude of −2.5 pA. Nicotinic acetylcholine receptor channel currents like these were seen in 24 of 91 cell-attached patch recordings made.

3.2. Channel current-voltage relationships

The channel currents like those shown in Fig. 3A and B were recorded at different pipette potentials, allowing the current-voltage relationship (Fig. 3C) to be determined. The slope (least squares fit) of the current-voltage plot in Fig. 3C gave a conductance of 45.1 ± 0.5 pS with a reversal potential close to 0 mV. The mean slope conductance measured from 16 patches ranged between 24.6–57.7 pS, and had a mean of 39.5 ± 2.0 pS.

Current-voltage plots from these channels were also recorded from isolated inside-out patches: the plots also had linear current-voltage relationships with all reversal potentials close to 0 mV. Because the predicted Nernst reversal potential for a cation-selective channel was 0 mV (symmetrical Cs^{+} across the isolated patch), and for a Cl^{-} channel it was −33 mV, we concluded that: (1) the channels we were recording from were permeable to Cs^{+}

and they were non-selective cation channels; (2) the membrane potential of the vesicles was close to zero. We were able to conclude that the membrane potential of the muscle vesicles was close to zero because the reversal potentials of channels recorded from the isolated inside-out patches were the same as that of the cell-attached patches. The membrane potentials of muscle vesicles prepared from *Ascaris* are also close to zero (Martin et al., 1990). Although the reason why the membrane potential of the vesicles collapses is not known, we concluded that the membrane potential of *O. dentatum* vesicles, like those of *Ascaris*, are equal but opposite in sign to the pipette potential applied to cell-attached patches.

3.3. Open-time distributions

Fig. 4A shows the distribution of open times observed in a cell-attached patch at a membrane potential of −50 mV. A single exponential was fitted to the distribution giving a mean open time of 2.3 ms. The mean open time recorded at −50 to −100 mV from patches ranged between 0.98–4.43 ms, and had a mean of 2.2 ± 0.2 ms, $n = 15$.

3.4. Closed-time distributions

The closed-time distributions were best fitted using three exponentials. Fig. 4B shows the closed-time distribution for the same experiment as in Fig. 3 and Fig. 4A displayed and plotted on a log-time scale. The three time constants of the closed distributions were: a fast component, t_1, 0.62 ms which produced the bursts and had an area of 0.366; an intermediate component, t_2, of 334 ms that had an area of 0.5; and a long component, t_3, of 1455 ms that separated the clusters of channel openings and which had an area 0.103. Of nine channels analysed, at potentials ranging between −50 and −100 mV, the mean duration of the t_1 was 0.68 ± 0.11 ms with an area of 0.43 ± 0.06 ms; the mean duration of t_2 was 23 ± 11 ms with an area of 0.13 ± 0.03; the mean duration of t_3 was 873 ± 150 ms with an area of 0.44 ± 0.06.

3.5. Burst distributions

Fig. 4C illustrates the burst distribution of the currents recorded from the same experiment as in Fig. 3 and Fig. 4A and B. The burst distribution was fitted with a single exponential with a time constant of 4.3 ms. The mean burst duration (−50 mV and −100 mV) recorded from eight patches was 4.57 ± 0.98 ms, $n = 8$.

3.6. The channel currents show differences in their conductances and mean open times revealing heterogeneity

Some channel recordings suggested the presence of more than one nicotinic channel: Fig. 5A shows a cell-attached recording at −75 mV where two separate channels were observed: there is a small amplitude (1.8 pA = 24.8 pS labelled S, Fig. 5A) and a large amplitude (3.3 pA = 43.8 pS labelled L, Fig. 5B). Histograms of the amplitudes of the open-channel currents from this experiment are fitted with two Gaussian distributions (Fig. 5B), further emphasizing the presence of two different channel types. The fact that direct transitions from one open level to another were very rare in this experiment suggests that the different conductance levels that we observed were not produced by a single type of nicotinic acetylcholine recep-

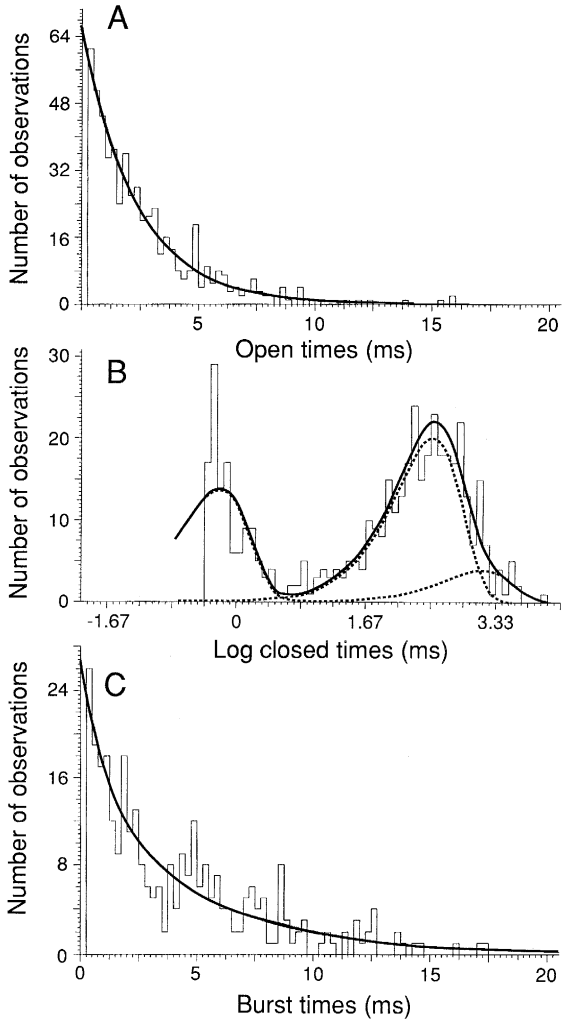

Fig. 4. Open-, closed- and burst-time distributions at −50 mV from the same experiment illustrated in Fig. 3. (A) Histogram and single exponential fit to open-time distribution. The mean open time was 2.3 ms. (B) Closed-time histogram plotted on a $\log_{10}$-time scale with the line fitting the three-exponential fit (solid line) and the separate components (dotted line). The three time constants of the closed-time distributions were: a fast component, t_1, 0.62 ms which had an area of 0.366; an intermediate component, t_2, of 334 ms that had an area of 0.5; and a long component, t_3, of 1455 ms that had an area of 0.103. (C) Burst-time distribution. Bursts were defined as a sequence of openings separated by a closing less than 3 ms in duration. One exponential was fitted to the burst distribution. The mean burst duration was 4.3 ms.

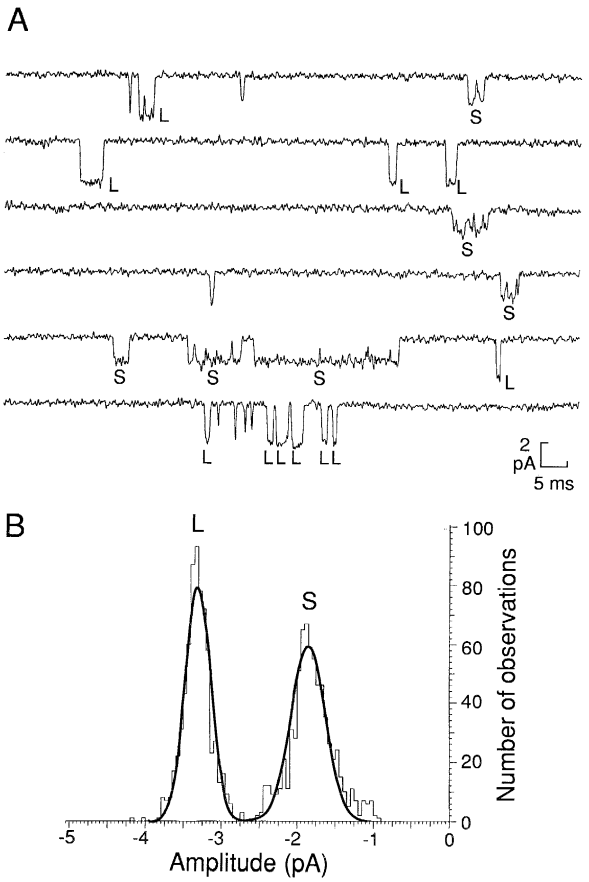

Fig. 5. (A) Cell-attached patch recording at −75 mV showing a small (S) and larger (L) nicotinic acetylcholine receptor channel present. (B) Amplitude histogram of open-channel amplitudes. Smaller conductance channel: mean current = −1.8 ± 0.2 pA (24.8 pS) labelled S (panel A). Larger conductance channel: mean current = −3.3 ± 0.2 pA (43.8 pS) labelled L (panel A). Histograms of the amplitudes of the open-channel currents were fitted with Gaussian distributions. 49% of the events were to the smaller amplitude, 51% were to the larger amplitude.

tor but rather two channels with similar but different properties. As a further test of the different properties of these two channels, we carried out a separate kinetic analysis on the two channel currents. We were able to separate these currents during analysis by editing because of the large difference in their amplitudes.

As a result of the kinetic analysis we found that the mean open time of the S channel was 2.27 ms and similar to the L channel, 2.33 ms. However, the mean burst duration of the S channel was 6.53 ms (Fig. 6A) and clearly longer than the L channel which was 4.07 ms (Fig. 6B). The longer burst duration of the S channel compared to the L channel is suggested in the sample of channel currents shown in Fig. 5A.

There were also differences in the closed-time kinetics. The S channel closed-time distribution was $t_1 = 0.68$ ms (area 0.546), $t_2 = 3.95$ ms (area 0.076), $t_3 = 1124$ ms (area 0.378). The L channel distribution was $t_1 = 0.65$ ms (area 0.371), $t_2 = 8.48$ ms (area 0.150), $t_3 = 545$ ms (area 0.479).

Fig. 7A is a histogram of all the channel conductances:

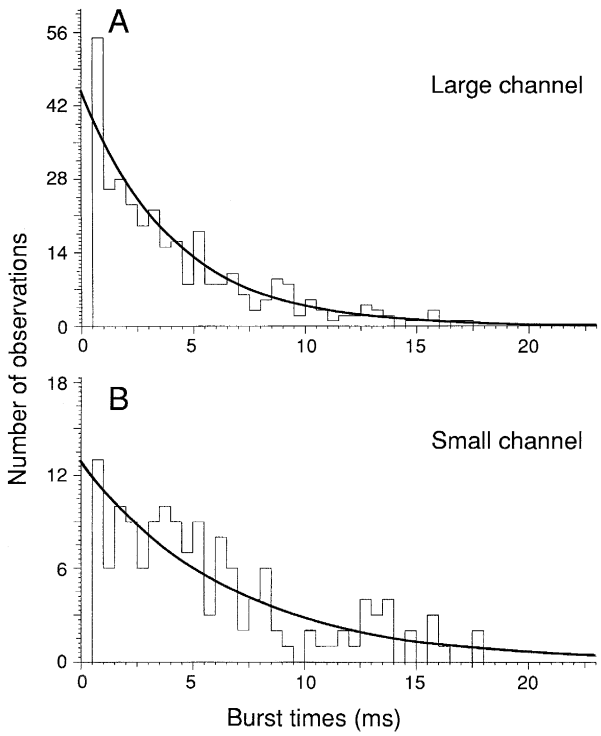

Fig. 6. Burst-time histograms of the smaller and larger channel shown in Fig. 5. The mean burst duration of the L channel was 4.07 ms (A), clearly smaller than the S channel value which was 6.53 ms (B).

it shows values which ranged between 24.6–57.7 pS; the presence of two main peaks at 35 pS and 45 pS; separated observations at 24.6 pS and 57.7 pS.

Fig. 7B is a frequency histogram showing the observed mean open times with ranges between 1.0–4.5 ms. It too shows the presence of two main peaks at 1.75 ms and 2.5 ms and again two separated observations. Fig. 7 implies that there are at least two main different types of nicotinic acetylcholine receptor present, each type characterized by a particular conductance and open time.

We separated out the channels with mean open times 1.25–2.00 ms and conductances 28.40–40.25 pS (designated the *G35* subtype because the mean conductance, *G*, was 35 pS), and the channels with mean open times 2.25–3.25 ms and conductances 43.80–45.60 pS (designated the *G45* subtype because the mean conductance was 45 pS) to determine their mean conductances and open times. The *G35* subtype had a mean conductance of 35.2 ± 1.8 pS and mean open time of 1.6 ± 0.1 ms, $n = 6$. The *G45* subtype had a mean conductance of 44.6 ± 0.35 pS

Table 1
Summary of mean ± S.E.M. values of the proposed levamisole receptor subtypes

Channel type	Conductance (pS)	Mean open time (ms)
G25	24.6	2.27
G35	35.2 ± 1.8	1.6 ± 0.1
G45	44.6 ± 0.35	2.7 ± 0.2
G55	57.7	0.98

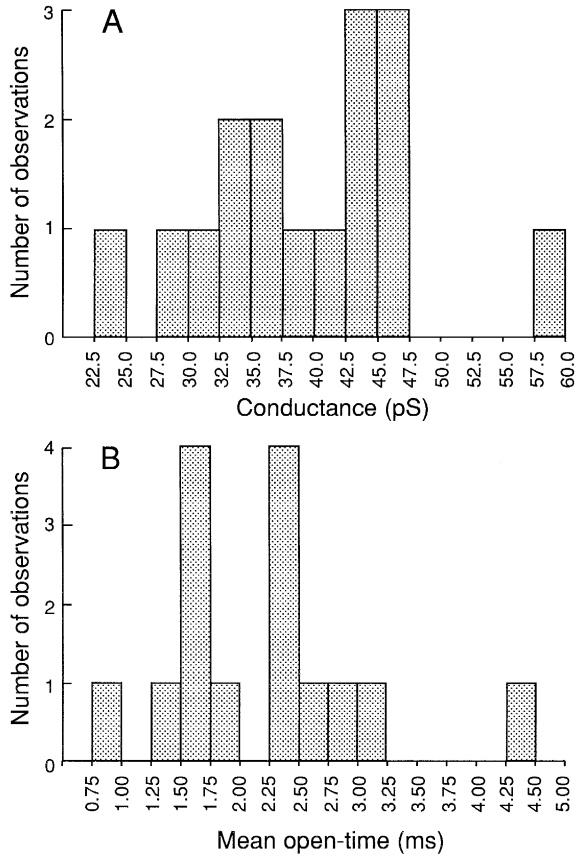

Fig. 7. (A) Frequency histogram of the channel conductances from different patches. Bin width 2.5 pS. Note the presence of two main peaks and two outliers. (B) Frequency histogram of the mean open times. Note the presence of two main peaks and two outliers. The total number of observations is one less in panel B than in panel A because of the limited frequency of channel openings observed at −50 or −75 mV in one recording.

and mean open time of 2.7 ± 0.2 ms, $n = 6$. Open times and conductances of *G35* and *G45* were significantly different (conductances, $P = 0.002$; mean open times, $P = 0.0002$). The presence of channels with properties outside the range of the properties of *G35* and *G45* (Fig. 7) suggests the presence of additional subtype groups. The 24.6 pS channel had a conductance that appeared less than the *G35* group but had a mean open time of 2.3 ms; the 57.7 pS channel had a conductance that apeared to be greater than the *G45* group and had a mean open time of 0.98 ms. Table 1 summarizes the properties of the subtypes of channel.

4. Discussion

The nicotinic acetylcholine receptors of nematode muscle have a pharmacological profile resembling mammalian neuronal nicotinic acetylcholine receptors (Colquhoun et al., 1991). For example, dimethylphenylpiperazinium is an agonist and mecamylamine is an antagonist at both receptors. Initially, in this discussion we refer to the heterogeneous nature of neuronal nicotinic acetylcholine receptors, and then argue that the nicotinic receptors of nematodes may be similar. The presence of heterogeneous nicotinic acetylcholine receptors in nematodes may provide a mechanism for the development of anthelmintic resistance.

4.1. Structure of vertebrate neuronal nicotinic receptors

The structure of the *Torpedo* electric organ nicotinic acetylcholine receptor is a pentamer of homologous subunits known as α, β, γ, δ with a stoichiometry of 2:1:1:1 (Changeau et al., 1996); the subunits are arranged like barrel staves around a central cation-selective ion channel. Although the stoichiometric structures of most mammalian neuronal nicotinic acetylcholine receptors are not known, they are often assumed to be a similar pentameric structure arising from the co-expression of 2α and 3β subunits (Lindstrom et al., 1987) but multiple stoichiometries (5α, 4α:1β, 3α:2β, 2α:3β, 1α:4β) or different arrangements around the ion-channel pore (e.g., ααβββ vs. αβαββ) are possibilities (McGehee and Role, 1995). Families of genes for neuronal α and β subunits exist: currently seven α subunits and three β subunits are recognised (McGehee and Role, 1995). The different α and β subunits are denoted by different subscript numbers (α_1, α_2, α_3; β_2, β_3, β_4). If the stoichiometry and subunit combination of a neuronal nicotinic acetylcholine receptor were known it might be specified as $2\alpha_3 3\beta_2$. However, the stoichiometry is not known and expressed receptors are referred to without reference to the stoichiometry of the subunit combination ($\alpha_3\beta_2$).

4.2. The pharmacology of the neuronal nicotinic acetylcholine receptors varies with subunit composition

Although the pharmacological profile of neuronal nicotinic acetylcholine receptors can vary with the molecular structure of the α subunit, it is also influenced by the β subunit structure. Expressed $\alpha_3\beta_2$ and $\alpha_3\beta_4$ have different macroscopic dose-response relationships, with $\alpha_3\beta_2$ showing a lower agonist dissociation constant and a more shallow dose-response curve (smaller Hill coefficient) than $\alpha_3\beta_4$ receptors: dimethylphenylpiperazinium is about 10 × more potent as an agonist on the $\alpha_3\beta_2$ receptors than the $\alpha_3\beta_4$ receptors (Covernton et al., 1996). Agonist binding sites are thought to be formed at specific subunit interfaces with the α subunit and adjacent unit (Karlin and Akabas, 1995) so that pharmacological differences can occur as the β subunit composition changes.

4.3. Biophysical properties of neuronal nicotinic acetylcholine receptors show heterogeneity

Single-channel studies on neuronal nicotinic acetylcholine receptors in sympathetic neurones (Mathie et al., 1991), habenula neurones (Connolly et al., 1995) or on $\alpha_3\beta_2$ or $\alpha_3\beta_4$ expressed in *Xenopus* oocytes (Papke et al.,

1996; Papke and Heineman, 1996) have shown that their channels have conductances and kinetics which vary dramatically from patch to patch. For example, the sympathetic nicotinic acetylcholine receptors have conductances constant in individual patches, but they vary from 26 to 48 pS between patches (Mathie et al., 1991). The expressed $\alpha_3\beta_2$ nicotinic acetylcholine receptors produce channels with conductances between 4–18 pS and were grouped into two main conductances (Papke et al., 1996). When an increased proportion of the cRNA for the β_2 was injected into the oocyte there was an increase in the proportion of patches where small conductance channels were observed, suggesting that the stoichiometry of α_3 to β_2 subunits could vary (Papke et al., 1996). The $\alpha_3\beta_4$ receptors had conductances that ranged between 11–24 pS and could be grouped into three main conductances which showed kinetic differences (Papke and Heineman, 1996).

Thus heterogeneity of the receptors produced by a variation in structure, arrangement or stoichiometry of the subunits making up the pentameric channel can lead to a variation in the pharmacological and biophysical properties of nicotinic acetylcholine receptors (McGehee and Role, 1995). The diversity of the neuronal nicotinic channels appears to arise from the differential or developmentally regulated expression of related genes (McGehee and Role, 1995).

4.4. Heterogeneity of O. dentatum nicotinic acetylcholine receptors

In this study of the muscle nicotinic acetylcholine receptors we have seen that the single channels can have conductances and mean open times that show significant variation between patches. The variation in conductance is far wider than expected from experimental errors or open-channel noise and is greater than that produced by vertebrate muscle nicotinic acetylcholine receptors (Garner et al., 1984). Such variation has been correlated with heterogeneity of the structure and pharmacology of vertebrate neuronal nicotinic acetylcholine receptors. In this study we were able to distinguish two main groups, *G35* and *G45*, of levamisole-activated channels on the basis of the conductance and mean open time of the channels. We also found evidence of additional nicotinic acetylcholine receptor subtypes (*G25* and *G55*). Heterogenous nicotinic acetylcholine receptor channel currents from *Ascaris suum*, with conductances ranging between 19–50 pS and distinguishable peaks at 24 pS and 42 pS, have been observed (Pennington and Martin, 1990; Robertson et al., 1994) but discrimination of the subtypes was less clear, perhaps because of variations in the source of the *Ascaris* that were derived from field infections.

4.5. Nicotinic acetylcholine receptor subunit genes in nematodes predict heterogeneity of levamisole receptors

Three genes encoding nicotinic acetylcholine receptor subunits in the model soil nematode, *C. elegans*, associated with levamisole resistance are *unc-38*, *unc-29* and *lev-1* (Lewis et al., 1980; Fleming et al., 1997). *Unc-38* encodes an α subunit while the *unc-29* and *lev-1* encode β subunits. Pairwise expression of *unc-38* and *unc-29* or *unc-38* and *lev-1* or co-expression of all three subunits in *Xenopus* oocytes results in levamisole-induced currents but *unc-38* expressed alone does not produce levamisole-activated currents. These observations suggest that the levamisole receptor cannot be comprised of a homo-oligomer of *unc-38* subunits and that channels are formed from a heterologous subunit combination.

Fig. 8 illustrates the eight possible arrangements of

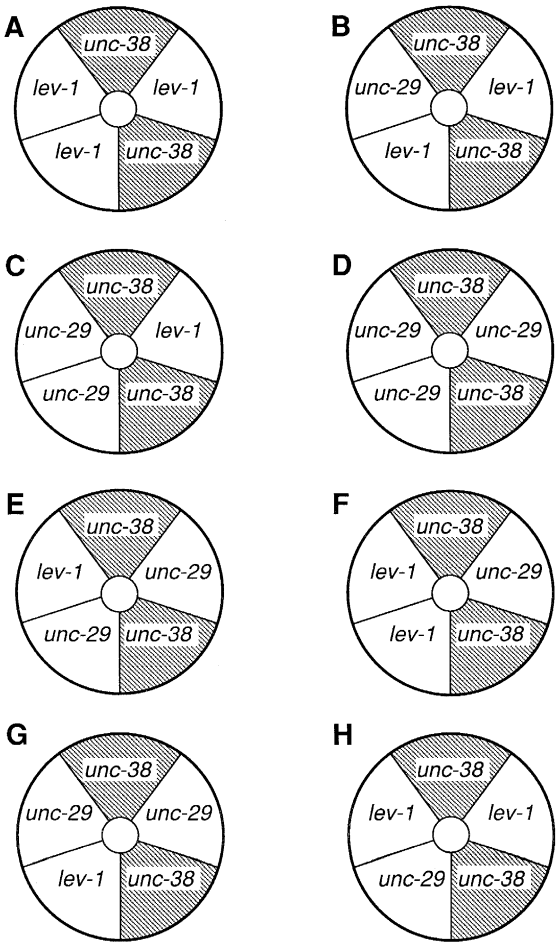

Fig. 8. Diagram of some possible subunit arrangements of *unc-38*, *unc-29* and *lev-1* subunits forming the nematode nicotinic acetylcholine receptor channel sensitive to levamisole. The *unc-38* is equivalent to the α subunit of vertebrate nicotinic channels. The *unc-29* and *lev-1* subunits are equivalent to vertebrate β subunits. The diagram shows that there are up to eight different combinations possible if two *unc-38* subunits are non-adjacent. If the conductance of the channel were determined only by the number of *unc-29* or *lev-1* subunits present in this scheme (assuming interactions between adjacent subunits do not affect overall channel conductance) then four distinct channel types would be distinguished on a basis of channel conductance (C has the same stoichiometry as E and G but the subunits are rearranged. B has the same stoichiometry as F and H but the subunits are rearranged. The diagram also illustrates that if the binding of the agonist molecule is at the interface of the *unc-38* subunit and an adjacent molecule then the binding of the agonist (including levamisole) will depend on subunit composition.

unc-38, *unc-29*, and *lev-1* with two *unc-38* subunits fixed in position but with eight possible variations in the position of the β subunits. If a functional channel could be produced with 1–5 *unc-38* subunits then there would be 3^4 (81) different receptor configurations. These receptors might be differentiated by their biophysical or pharmacological properties with the conductances being determined by the subunits making up the channel pore and the agonist binding sites being determined by the interfaces between the *unc-38* subunit and adjacent units. Fig. 8, for example, shows four different stoichiometric combinations (but with different arrangements) of the subunits and predicts the existance of four nicotinic acetylcholine receptor subtypes distinguished by evenly spaced conductance intervals (e.g., *G25*, *G35*, *G45* and *G55*) as we have observed here. However, it is pointed out that this model may be oversimplified, ignoring interactions between adjacent subunits that affect the overall conductance of the channel.

4.6. Development of anthelmintic resistance

The properties of vertebrate neuronal receptors show us that potency of different agonists at nicotinic acetylcholine receptors varies with the subunit structure of the channel (e.g., Covernton et al., 1996). It is reasonable to imagine that the sensitivity of a strain of nematode parasites to a nicotinic anthelmintic like levamisole may also depend upon the pattern of subunit expression of the muscle nicotinic receptors. An increase in expression of one subunit combination may increase the required therapeutic dose of levamisole. The expression of different subunits in nematodes may arise from the continued presence of levamisole in the environment in the same way as the density of particular subunit stoichiometry increases in the human brain after chronic exposure to nicotine (Peng et al., 1994) if the nematode species can survive; or it may increase as a results of selection pressure as a result of clonal expansion.

Acknowledgements

We are pleased to acknowledge the financial support of the Wellcome Trust. Ref. 043509/z/95/z/JRS/SH.

References

Aceves, J., Erliji, D., Martinez-Marnon, R., 1970. The mechanism of the paralysing action of tetramisole on *Ascaris* somatic muscle. Br. J. Pharmacol. 38, 602–607.

Bjorn, H., 1994. Workshop summary: Anthelmintic resistance. Vet. Parasitol. 54, 321–325.

Changeau, J.-P., Devillers-Thiery, A., Chemouilli, P., 1996. Acetylcholine receptor: an allosteric protein. Science 225, 1335–1345.

Colquhoun, L., Holden-Dye, L., Walker, R.J., 1991. The pharmacology of cholinoceptors on the somatic muscle-cells of the parasitic nematode *Ascaris-suum*. J. Exp. Biol. 158, 509–530.

Connolly, J.G., Gibb, A.J., Colquhoun, D., 1995. Heterogeneity of neuronal nicotinic acetycholine receptors in thin slices of rat medial habenula. J. Physiol. (London) 484, 87–105.

Covernton, P.J.O., Kojima, H., Sivilotti, L.G., Gibb, A.J., Colquhoun, D., 1996. Comparison of neuronal nicotinic receptors in rat sympathetic neurones with subunit pairs expressed in *Xenopus* oocytes. J. Physiol. (London) 481, 27–34.

Fleming, J.T., Baylis, H.A., Satelle, D.B., Lewis, J.A., 1997. Molecular cloning and in vitro expression of *C. elegans* and parasitic nematode ionotropic receptors. Parasitology (in press).

Garner, P., Ogden, D.C., Colquhoun, D., 1984. Conductances of single ion channels opened by nicotinic agonists are indistinguishable. Nature 309, 160–162.

Harrow, I.D., Gration, K.A.F., 1985. Mode of action of the anthelmintics morantel, pyrantel and levamisole on muscle-cell membrane of the nematode *Ascaris suum*. Pest. Sci. 16, 662–672.

Kao, C.Y., Karlin, A., 1996. Acetylcholine receptor binding site contains a disulfide cross link between adjacent half-cystinyl residues. J. Biol. Chem. 261, 8085–8088.

Karlin, A., Akabas, M., 1995. Towards a structural basis for the function of nicotinic acetylcholine-receptors and their cousins. Neuron 15, 1231–1244.

Lewis, J.A., Wu, C.-H., Levine, J.H., Berg, H., 1980. Levamisole-resitant mutants of the nematode *Caenorhabditis elegans* appear to lack pharmacological acetycholine receptors. Neuroscience 5, 967–989.

Lindstrom, J., Schoefpfer, R., Whiting, P., 1987. Molecular studies of the neuronal nicotinic acetylcholine receptor family. Pflüg. Arch. 1, 281–337.

Martin, R.J., 1980. The effect of γ-aminobutyric acid on the input conductance and membrane potential of *Ascaris* muscle. Br. J. Pharmacol. 71, 99–106.

Martin, R.J., Valkanov, M.A., 1996. Effects of acetylcholine on a slow voltage-activated non-selective cation-current mediated by non-nicotinic receptors on isolated *Ascaris* musle bags. J. Exp. Physiol. 81, 909–925.

Martin, R.J., Kusel, J.R., Pennington, A.J., 1990. Surface properties of membrane-vesicles prepared from muscle cells of *Ascaris suum*. J. Parasitol. 76, 340–348.

Mathie, A., Cull-Candy, S.G., Colquhoun, D., 1991. Conductance and kinetic properties of single nicotinic acetylcholine receptor channels in rat sympathetic neurones. J. Physiol. (London). 439, 717–750.

McGehee, D.S., Role, L.W., 1995. Physiological diversity of nictotinic acetylcholine receptors expressed by vertebrate neurons. Annu. Rev. Physiol. 57, 521–546.

Papke, R.L., Boulter, J., Patrick, J., Heinmann, S., 1996. Single channel currents of rat neuronal nicotinic acetylcholine receptors expressed in *Xenopus laevis* oocytes. Neuron 3, 589–596.

Papke, R.L., Heineman, F., 1996. The role of the β_4-subunit in determining the kinetic properties of rat neuronal nicotinic acetycholine α_4-receptors. J. Physiol. (London). 440, 95–112.

Peng, X., Anand, R., Whiting, P., Lindstrom, J., 1994. Nicotine-induced increase in neuronal nicotinic receptors results for a decrease in rate of receptor turnover. Mol. Pharmacol. 46, 532–530.

Pennington, A.J., Martin, R.J., 1990. A patch-clamp study of acetylcholine-activated ion channels in *Ascaris suum* muscle. J. Exp. Biol. 154, 210–221.

Prichard, R.K., 1994. Anthelmintic resistance. Vet. Parasitol. 54, 259–268.

Robertson, S.J., Martin, R.J., 1993. Levamisole-activated single-channel currents from muscle of the nematode parasite *Ascaris suum*. Br. J. Pharmacol. 108, 170–178.

Robertson, S.J., Pennington, A.J., Evans, A.M., Martin, R.J., 1994. The action of pyrantel as an agonist and an open channel blocker at acetylcholine receptors in isolated *Ascaris suum* muscle vesicles. Eur. J. Pharmacol. 271, 273–282.

Slotved, H.C., Barnes, E.H., Bjorn, H., Christensen, C.M., Eriksen, L., Roepstorff, A., Nansen, P., 1996. Recovery of *Oesophagostomum dentatum* from pigs by isolation of parasites migrating from large intestinal contents embedded in agar-gel. Vet. Parasitol. 63, 237–245.